On-going investigation of Japanese longline CPUE for yellowfin tuna in the Indian Ocean standardized by vector-autoregressive spatiotemporal model

K. Satoh[1], T. Matsumoto[2],
H. Yokoi[1] , K. Okamoto[2] and T. Kitakado[3]

[1]*Fisheries Resources Institute, Japan Fisheries Research and Education Agency, 2-12-4, Fukuura, Kanazawa-ku, Yokohama-shi, 236-8648, Japan*
[2]*Fisheries Resources Institute, Japan Fisheries Research and Education Agency, 5-7-1, Orido, Shimizu, Shizuoka, 424-8633, Japan*
[3] *Tokyo University of Marine Science and Technology, 5-7, Konan 4, Minato, Tokyo, 108-8477, Japan*

Abstract

Japanese longline CPUE for yellowfin tuna in the Indian Ocean (IO) was standardized for 1975-2020 by vector-autoregressive spatiotemporal model (VAST). Two types of abundance indices, size-aggregated index and size-specific index of yellowfin tuna in the IO were developed to address the shrinking fishing ground of Japanese longline fishery in the IO using VAST. Cluster analysis was conducted before standardization, and cluster number by sub area was used as a catability covariates in some models. The information about the cluster number was influential in the CPUE standardization process, which affected the time series. The cluster number (targeting effect) makes the decreasing trend of the time series of indices calm (flatten). In the eastern part of the IO, the smaller fish (age 2 and 3) distributed, while in the western part all size fish distributed, and the largest fish (age 5+) distributed southern part of the Mozanbique channel.

1. Introduction

Yellowfin tuna is one of main target species for Japanese longline fishery in the Indian Ocean (IO). Its abundance indices are very important for stock assessment of this species. After World War II, the Japanese longline fishery resumed fishing activity in the vicinity of Japan and then expanded to the IO since 1952. This fishery is still active in the IO as of 2020, but the expansion of fishing efforts stopped around the 1990s, being followed by a contraction in effort. Yellowfin tuna is mainly caught in the tropical and subtropical areas especially in the western IO (Matsumoto and Satoh, 2012; Matsumoto 2014). Since 2007, piracy activities off Somalia have increased and spread to whole northwestern IO. Japanese longline effort in the IO, especially in the northwestern part, has rapidly decreased to avoid the piracy attack. The geographical coverage of the fishery shrank drastically in recent years. Ignoring unfished areas (e.g., by assuming zero catch rate) could greatly bias the estimation of population depletion status (Walters, 2003). Therefore, a methodology using spatiotemporal information to impute population densities in unfished areas needs to be developed to provide a more reliable index of relative abundance. The vector-autoregressive spatiotemporal model (VAST; Thorson and Barnett 2017) can be applied to CPUE data to deal with the difficulty of standardizing fishery-dependent CPUE data by accounting for correlated spatial processes and predicting densities in unfished areas via imputation using an area-weighted approach.

A new collaborative study for developing the abundance index started in 2019 by Japanese, Korean and Taiwanese scientists has been conducted for analyzing CPUE for the IO yellowfin tuna (Kitakado et al., 2021). In this collaborative study, in addition to the traditional GLM methods, VAST will also be developed. However the developing of VAST model had faced a conversion problem thus the results of VAST were not included in the working paper of the collaborative work. This document reports on-going analysis of the standardization of Japanese longline CPUE for yellowfin tuna in the IO using VAST appling to only Japanese longline data instead of three countries combined data. The results may help to think about an application of these CPUE indices to stock assessment model especially for the size (age) specific indices.

The aims of this study were 1) to develop two types of abundance indices, size-aggregated index and size-specific index of yellowfin tuna in the IO that address the shrinking fishing ground of Japanese longline fishery in the IO using spatiotemporal models (VAST), 2) to describe the size-specific spatiotemporal distribution of yellowfin in the IO although it is an on-going study.

2. Materials and methods

Catch and effort (CE) data ans size composition data used:

Japanese longline catch and effort records (logbook) and size composition data are stored and updated continuously by the Highly Migratory Resources Division, Fisheries Resources Institute, National Research and Development Agency, Japan Fisheries Research and Education Agency (FRA). This institution's predecessor is the National Research Institute of Far Seas Fisheries, Fisheries Research Agency (NRIFSF), Japan. The data updated as of January 2021 were used in this study. The logbook and size composition data were available from 1952 to 2020, and from 1948 to 2019, respectively.

Operational level (set by set) Japanese longline logbook data with vessel ID were used. The data were available for 1975-2020 (data for 2020 were preliminary). The data include the fields year, month and day of operation, location to 1° of latitude and longitude, vessel identifier (call sign and vessel registration number), number of hooks between floats (HBF), number of hooks per set, and catch in number of each species. In the previous collaborative studies, vessel ID was available from 1979, but currently the information for longer period (from 1975) is available. Each set was allocated to subregion (subarea) (**Fig. 1**).

The size composition data with fine spatial resolution (1 × 1° square), which best approximated the resolution of the logbook data, is only available after 1986. Thus the period for a size-specific index used in this study is from 1986 to 2019. Fish size was measured on board by fisherman and/or observer using a straight caliper. These two data sets (CE and size composition data) are aggregated in monthly intervals and 1 × 1° square, and then merged after applying for the cluster analysis. The month- 1 × 1° square cells that lack size composition data are removed from VAST model input data. The coverages of CE data with the size composition data in catch and cell (1 × 1° square) number were around several % in recent years with annual fluctuation (**Fig. 2**), and there was luck of data in a specific area (**Fig. 1**), however the merged data still cover the IO. Fish body size is categorized into 4 groups according to the yellowfin tuna growth schedule in Fonteneau (2008): age 2 (FL > 65 cm and FL =< 106 cm), age 3 (FL > 106 cm and =< 127 cm), age 4 (FL > 127 cm and =< 137) and age 5+ (FL > 137 cm).

Cluster analysis

We clustered the data using the approach described by Kitakado et al. (2021), which used Ward's minimum variance and the complete linkage methods. Species composition in number of the catch was aggregated for 10-days period (1st-10th, 11th-20th, and 21st~ for each month), and was used for cluster analysis. Catch for southern bluefin tuna (SBT), albacore (ALB), bigeye tuna (BET), yellowfin tuna (YFT), swordfish (SWO), sharks (SKX) and other fish (OTH) were used for species composition. Data were also clustered using the kmeans method, which minimises the sum of squares from points to the cluster centres.

Vector-autoregressive spatiotemporal model (VAST):

After cluster analysis, cluster numbers were assigned to Ct data aggregated by year, month, vessel ID and 1 degree latitude/longitude blocks. This data set was used for CPUE standardization. A vector-autoregressive spatiotemporal delta-generalized linear mixed model was applied to catch and effort data for yellowfin tuna using the open-source spatiotemporal R package VAST (Thorson and Barnett, 2017). The methodology of this model is almost the same as a previous study (Xu et al*.,* 2019) except allowing for processes to differ among fish size groups and including the cluster number catchability covariates. The delta-generalized linear mixed model method decomposed the catch rate into the probability of positive catch (encounter probability) and the positive catch rate (Maunder and Punt, 2004). In this study, we model the encounter probability (p_1), in the delta model for observation *i* using a logit-link linear predictor:

$$logit(p_1(i)) = \beta_1(l_i, t_i) + \sum_{f=1}^{n_{\omega 1}} L_{\omega 1}(l_i, f)\omega_1(s_i, f) + \sum_{f=1}^{n_{\varepsilon 1}} L_{\varepsilon 1}(l_i, f)\varepsilon_1(s_i, f, t_i) +$$

$$\sum_{f=1}^{n_{\eta 1}} L_1(l_i, f)\eta_1(v_i, f) + \lambda_1 Q(i) \quad (1)$$

and model the positive catch rate (p_2) in the delta model for observation *i* using log-link linear predictor:

$$log(p_2(i)) = \beta_2(l_i, t_i) + \sum_{f=1}^{n_{\omega 2}} L_{\omega 2}(l_i, f)\omega_2(s_i, f) + \sum_{f=1}^{n_{\varepsilon 2}} L_{\varepsilon 2}(l_i, f)\varepsilon_2(s_i, f, t_i) +$$

$$\sum_{f=1}^{n_{\eta 2}} L_2(l_i, f)\eta_2(v_i, f) + \lambda_2 Q(i) \quad (2)$$

where l_i is the fish size category for each sample *i*, $\beta(l_i, t_i)$ is an intercept for fish length category l_i in year t_i,

$L_\omega(l_i, f)$ is the impact of each factor f on each fish length category l_i in the loading matrix L_ω, $\omega(s_i, f)$ is a vector of random effects that has a mean of zero and standard deviation of 1.0, representing unmeasured spatial variation at location (knot) s_i, as represented by factor *f*, $L_\varepsilon(l_i, f)$ is the impact of each factor *f* on each fish length category l_i in the loading matrix L_ε, $\varepsilon(s_i, f, t_i)$ is a vector of random effects, representing unmeasured spatio-temporal variation at location s_i as represented by factor *f*, $L(l_i, f)$ is the impact of each factor f on each fish length category l_i in the loading matrix in the loading matrix L, $\eta(v_i, f)$ is a vector of random effects that has a mean of zero and standard deviation of 1.0, representing vessel effect, λ is the impact of the catchability covariate, $Q(i)$ is catchability covariate variables (cluster number) for each observation. Vessel effects are included in the spatiotemporal model to capture differences in fishing power among vessels as vessel name, however for some models the vessel name (v_i) for each observation was altered as vessel name + sub-area + cluster number, in these cases the catchbility covariates were not included. In this analysis, the levels of factor *f* is hypothesized to be two or three for the four model components, spatial and spatio-temporal variation for both linear predictors, except for the spatial variation in the encounter probability. The intercept for each linear predictor (β_1 and β_2) is a fixed effect for each year, which ensures that the estimates of abundance are independent for each modeled year. It is a default setting of VAST and is appropriate one when estimating an abundance index to be used for stock assessment (Thorson 2019). The spatio-temporal random effect *ε1* and *ε2* are also assumed independent among years, Spatial variation represents a species' expected spatial distribution on average over time, whereas spatio-temporal variation represents a species' environmental response to unmeasured environmental conditions (Thorson 2019).

The probability function for observed CPUE (c_i) is

$$\Pr(c_i = c) = \begin{cases} 1 - p_1(i) & \text{if } c = 0 \\ p_1(i) \times Lognormal\{c_i = c_i | \log(p_2(i), \sigma^2\} & \text{if } c > 0 \end{cases} \quad (3)$$

where σ^2 is a dispersion parameter for the positive catch rate. The population density $d(s, l, t)$ for each location *s*, fish length category *l*, and time *t* are predicted from both linear predictors when the terms affecting catchability are dropped:

$$d(s,l,t) = logit^{-1}\left(\beta_1(l_i,t_i) + \sum_{f=1}^{n_{\omega 1}} L_{\omega 1}(l_i,f)\omega_1(s_i,f) + \sum_{f=1}^{n_{\varepsilon 1}} L_{\varepsilon 1}(l_i,f)\varepsilon_1(s_i,f,t_i)\right) \times exp\left(\beta_2(l_i,t_i) + \sum_{f=1}^{n_{\omega 2}} L_{\omega 2}(l_i,f)\omega_2(s_i,f) + \sum_{f=1}^{n_{\varepsilon 2}} L_{\varepsilon 2}(l_i,f)\varepsilon_2(s_i,f,t_i)\right) \quad (4)$$

The abundance index $Index(l, t)$ of yellowfin tuna for fish length category *l* in time *t* is then calculated from the predictions of local density using an area-weighted approach:

$$Index(l,t) = \sum_{s=1}^{n_s} (a(s) \times d\,(s,l,t)) \quad (5)$$

where n_s is the number of knots, $a(s)$ is the area associated within knot s used to weight the density estimates at different knots, and $d\,(s, l, t)$ is the predicted density for knot *s*, fish size category *l* and year *t*. For computational purposes, we used the k-means algorithm to cluster all the grid cells into 500 spatial knots (**Fig. 3**).

3. Results and discussion

Spatiotemporal models successfully converged except for the VC model and the size-base model (**Table 1**), which were confirmed by maximum gradient components less than the criteria of 0.0001. The maximum gradient components of 0.0004 for the VC model was near the criteria. The base model was converged however its standard error of abundance indieces were large, more than 20 – 200 times of the index. For the diagnostic of a gooness of fit for the encounter rates indicated that the size-aggregated models were fine while there were room of improvement for the size specific models showing some discrepancy (**Fig. 4**).

Size-aggregated index

Time series of the standardized indices of the size-aggregated models by sub-area showed decreasing trend in all aub-

area from 1975 to 2020 exept for the sub-area R3. In the R3 the standardized index was stable after around 2000. The standardized CPUEs were less fluctuated than the nominal one (**Fig. 5**). In the R3 there was also bias between the two time series. The time series of nominal CPUEs showed continuous increasing trend after 1990, while the standardized indices were stable after around 2000. The V model excluding the cluster number information showed larger standardized CPUE values pre-around 2000 and lower values post-2000 than the other two models (base and VC models), which indicated that the cluster number (targeting effect) makes the decreasing trend of the time series of indices calm (flatten) (**Fig. 8**). The geographic distribution of mean predicted log density from 1975 to 2020 of the base and VC model was similar, however that of the V model was different with those of the other two models, which showe higher densities in the Mozanbique channels. The information about the cluster number was influential in the CPUE standardizationmodel that affected the time series and the geographical distribution.

Size (age)-specific index

It seems that the time series of the standardized CPUEs of the larger than the age 3 fish were similar to each other however the CPUEs of the smallest fish (age 2) were more fluctuated than the other size fishes (**Figs. 6 and 7**). When comparing the time series between the excluding cluster number information model (the V model) and the VC model (including the cluster number information), the larger standardized CPUE values pre-around 2000 and lower values post-2000 were found in the size-V model in all sub-area and all age (**Fig. 9**). Although there were differences among models (the V and VC models), there were a spatial segregation by fish body size in the IO. In the eastern part of the IO, the smaller fish (age 2 and 3) distributed, while in the western part all size fish distributed, and the largest fish (age 5) distributed southern part of the Mozanbique channel **(Fig. 11)**. The time lag among the size (age)-specific was not clear (**Fig. 12**).

The difference of time series in the size (age)- specific index and the segregation of spatial distribution were found although the development of the spatio-temporal model of the VAST model is on-going. We need further analysis to solve several problems including the large standard error of the index of the base model and the fit of the encounter rates. We also should develop a protocol to apply the age-specific indices to the stock assessment model in the future.

4. References

Kitakado T., K. Satoh, Sl Lee , NJ Su, T Matsumoto, H Yokoi, K Okamoto, MK Lee, JH Lim, Y Kwon, SP Wang, WP Tsai, ST Chang, and FC Chang. (2021) Report of trilateral collaborative study among Japan, Korea and Taiwan for producing joint abundance indices for the yellowfin tunas in the Indian Ocean using longline fisheries data up to 2019. IOTC-2021-WPTT23DP-XX.

Matsumoto, T. (2014): Review of Japanese fisheries and tropical tuna catch in the Indian Ocean. IOTC 2014/WPTT16/10. 28pp.

Matsumoto, T. and Satoh, K. (2012): Review of Japanese fisheries and tropical tuna catch in the Indian Ocean. IOTC 2012/WPTT14/17. 28pp.

Maunder, M.N., Punt, A.E., (2004): Standardizing catch and effort data: a review of recent approaches. Fish. Res. 70 (2-3), 141–159.

Thorson, J.T., (2019): Guidance for decisions using the vector autoregressive spatio-temporal (VAST) package in stock, ecosystem, habitat, and climate assessment. Fish. Res. 210, 143–161. 10.1016/j.fishres.2018.10.013.

Thorson, J.T., Barnett, L.A.K., (2017): Comparison of estimates of abundance trends and distribution shifts using single- and multispecies models of fish and biogenic habitats. ICES J. Mar. Sci. 74 (5), 1311–1321.

Walters, C., (2003): Folly and fantasy in the analysis of spatial catch rate data. Can. J. Fish. Aquat. Sci. 60 (12), 1433–1436.

Xu, H., Lennert-Cody, C., Maunder, M.N., Minte-Vera, C., (2019): Spatiotemporal dynamics of the dolphin-associated purse-seine fishery for yellowfin tuna (Thunnus albacares) in the eastern Pacific Ocean. Fish. Res. 213, 121–131.

10.1016/j.fishres.2019.01.013.

Table 1. Sumamry of convergence and setting of vessel effect and catchability covariates (cluster number; target effect) of each model. The default criteria for convergence is less than 0.0001 in this study. Base model is a model including both the catchability covariates and vessel effect. The VC model is a model including only the vessel effect but the vessel effect included the cluster number information as "vessel name + sub area + cluster number". V mdodel is a model not including the catchability covariates but the vessel effect only.

Vessel effect	Vessel name	Vessel name + sub area + cluster number	Vessel name
Catchability covariates	Cluster number (target effect) by sub area	【Information of cluster number is included in the vessel name】	Not included
Size aggregated model (one index)	Base model There is no evidence that the model is not converged (maximum gradient 1.295534e-05). The standard error of index was large.	VC model The model is likely not converged (maximum gradient 0.0004193966).	V model There is no evidence that the model is not converged (maximum gradient 2.904013e-05).
Size specific index (four incises according to age 2, 3, 4 and 5+)	Size-base model No results	Size-VC model There is no evidence that the model is not converged (maximum gradient 1.95461e-07).	Size-V model There is no evidence that the model is not converged (maximum gradient 7.501811e-07).

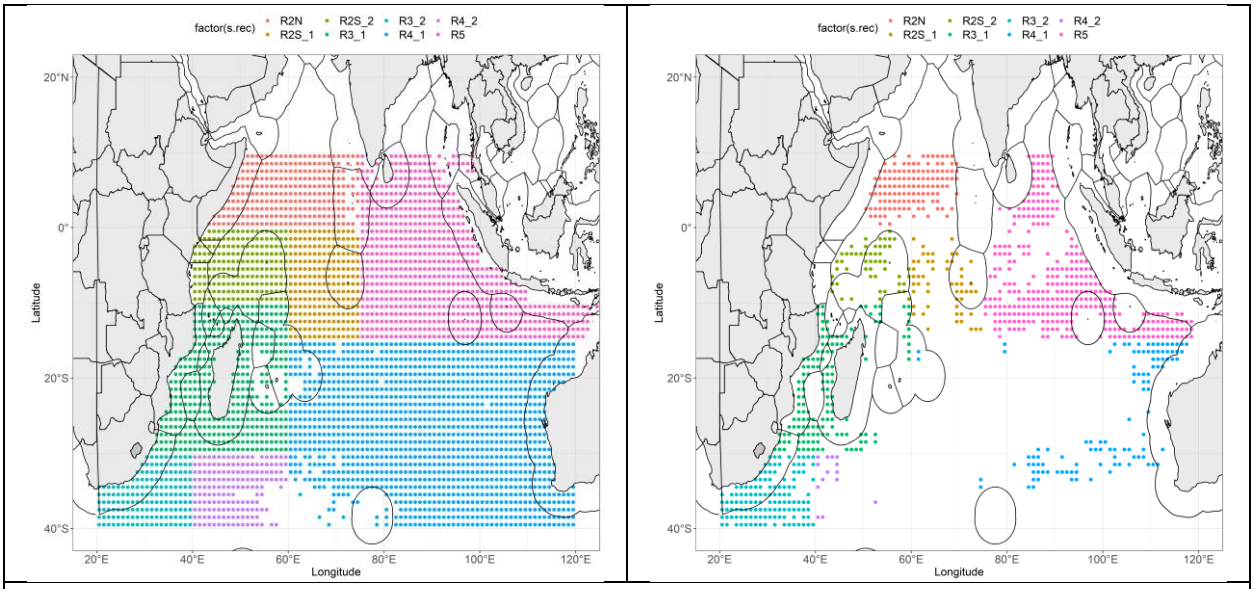

Fig. 1. Definition of areas and data points used in this study.
For the size aggregated model (left), for the size-specific model (right). The data point of the size specific model is based on the merged data (catch and effort data with size composition data).

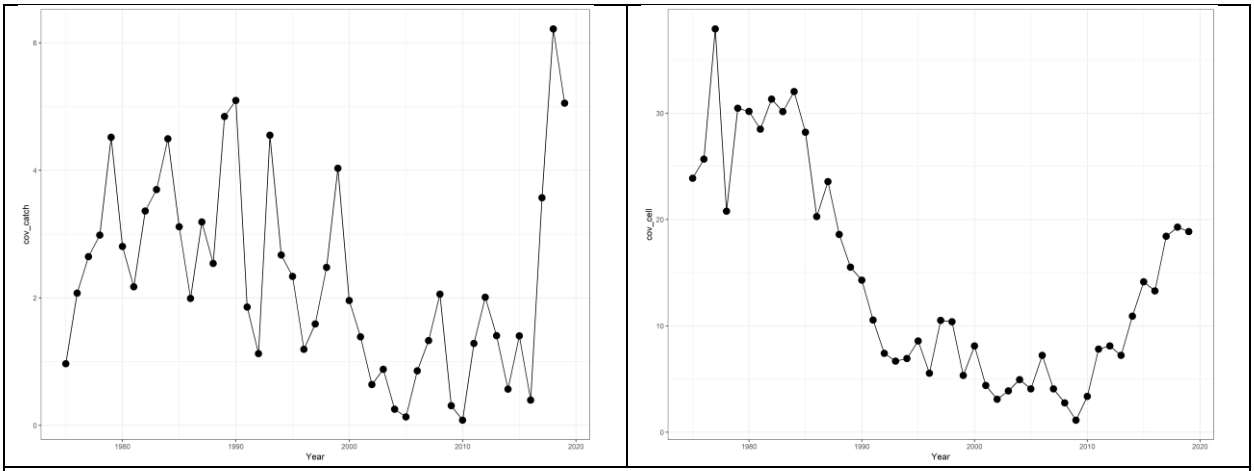

Fig. 2. Coverage of catch and effort data with the size composition data comparing to original catch and effort data. Catch amount coverage (left) and the cell (1 × 1° square) number coverage (right) from 1986 to 2019.

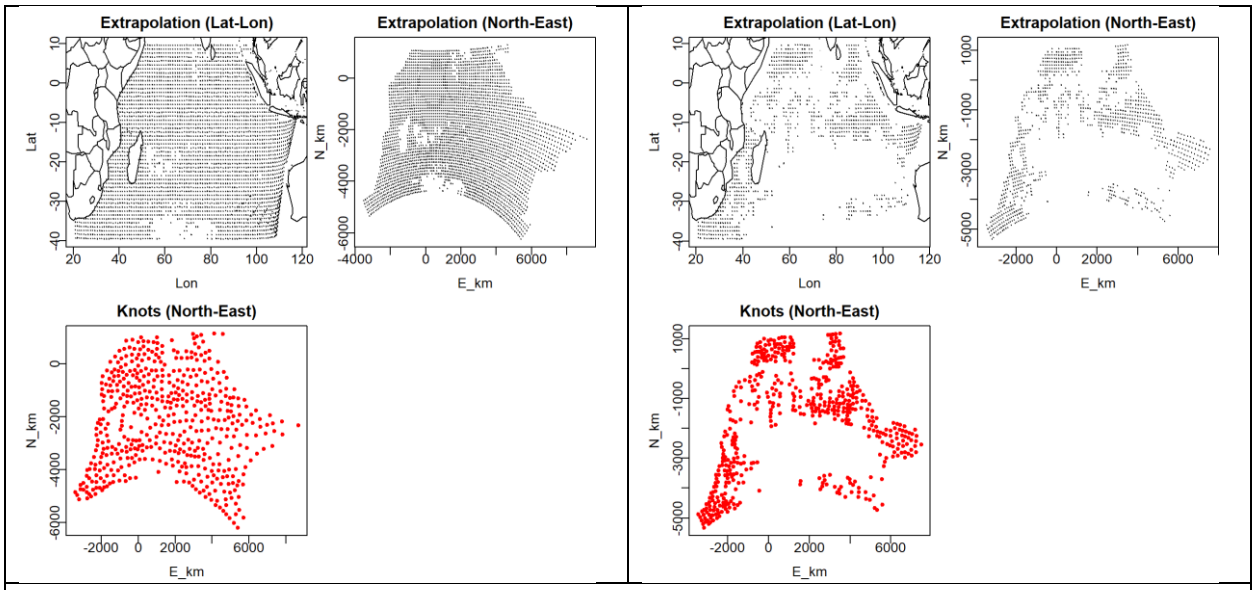

Fig. 3. Data points used in VAST analysis.
For the size aggregated model (VC model, left three panels), for the size-specific model (size-VC model, right three panels). The locations of knots (red dots in bottom left panels of each model) were corresdonding to the data points (upper right panels of each model).

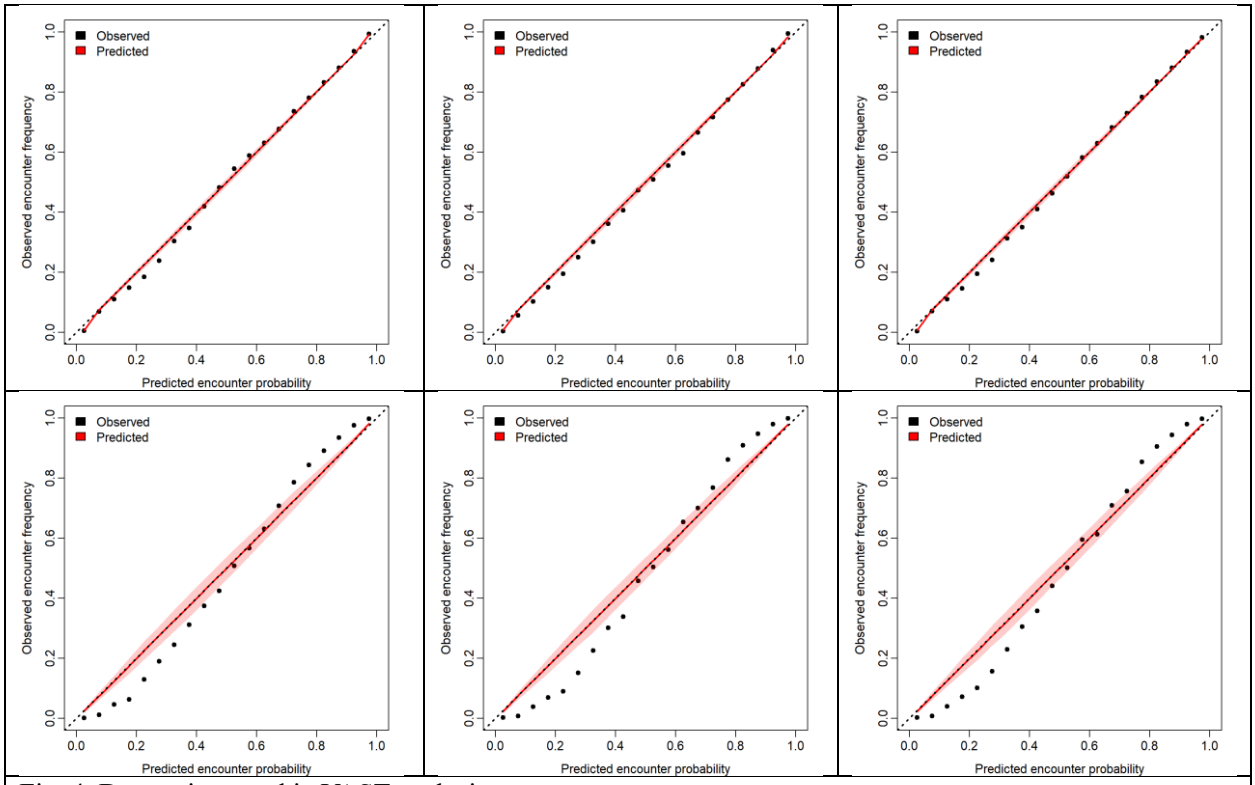

Fig. 4. Data points used in VAST analysis.
For the size aggregated model (upper; Base, VC and V model from left to right), for the size-specific model (bottom; size- Base, size-VC and size-V model from left to right). The diagnostics for the size specific model indicated that there is a room of improvement.

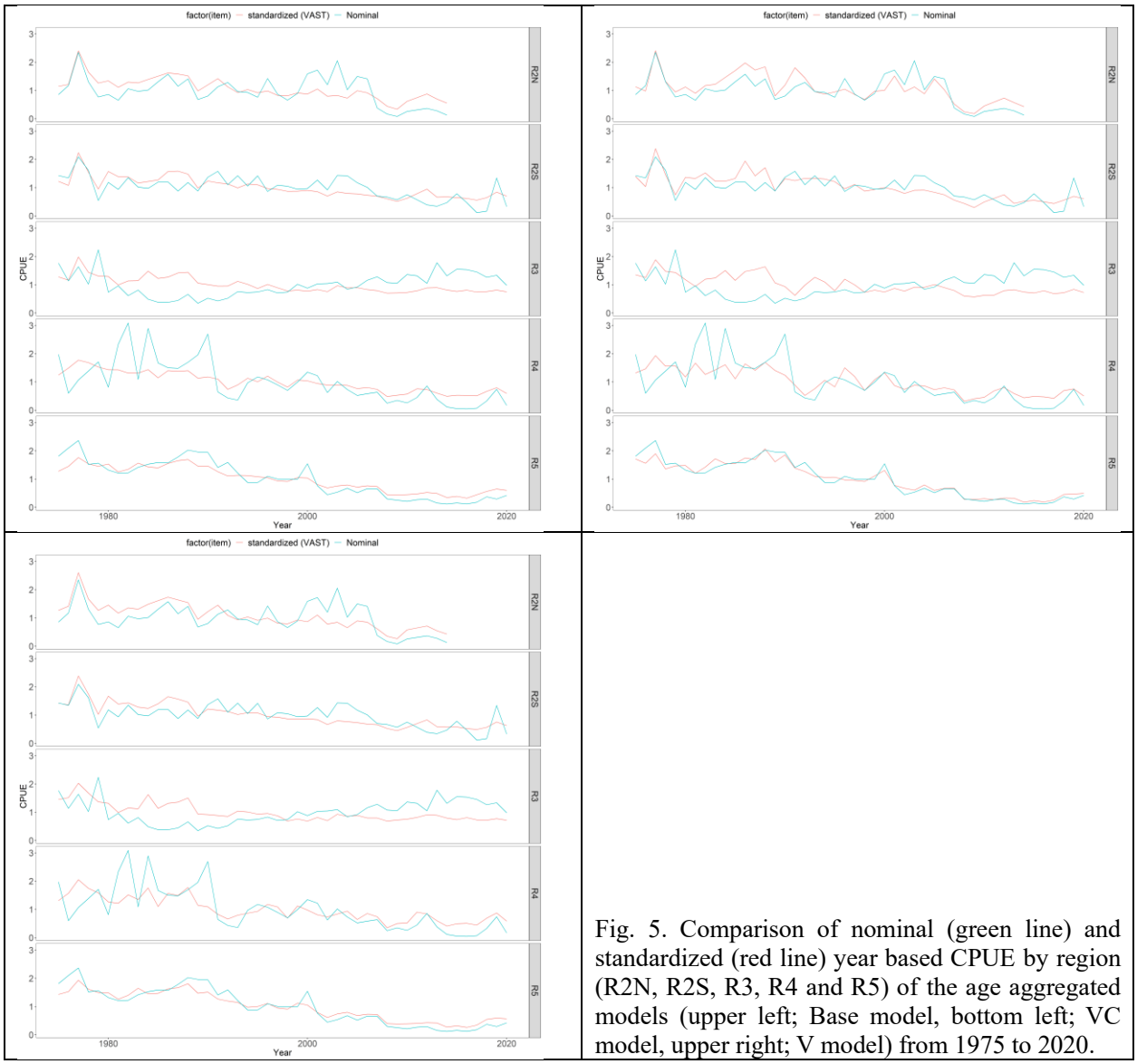

Fig. 5. Comparison of nominal (green line) and standardized (red line) year based CPUE by region (R2N, R2S, R3, R4 and R5) of the age aggregated models (upper left; Base model, bottom left; VC model, upper right; V model) from 1975 to 2020.

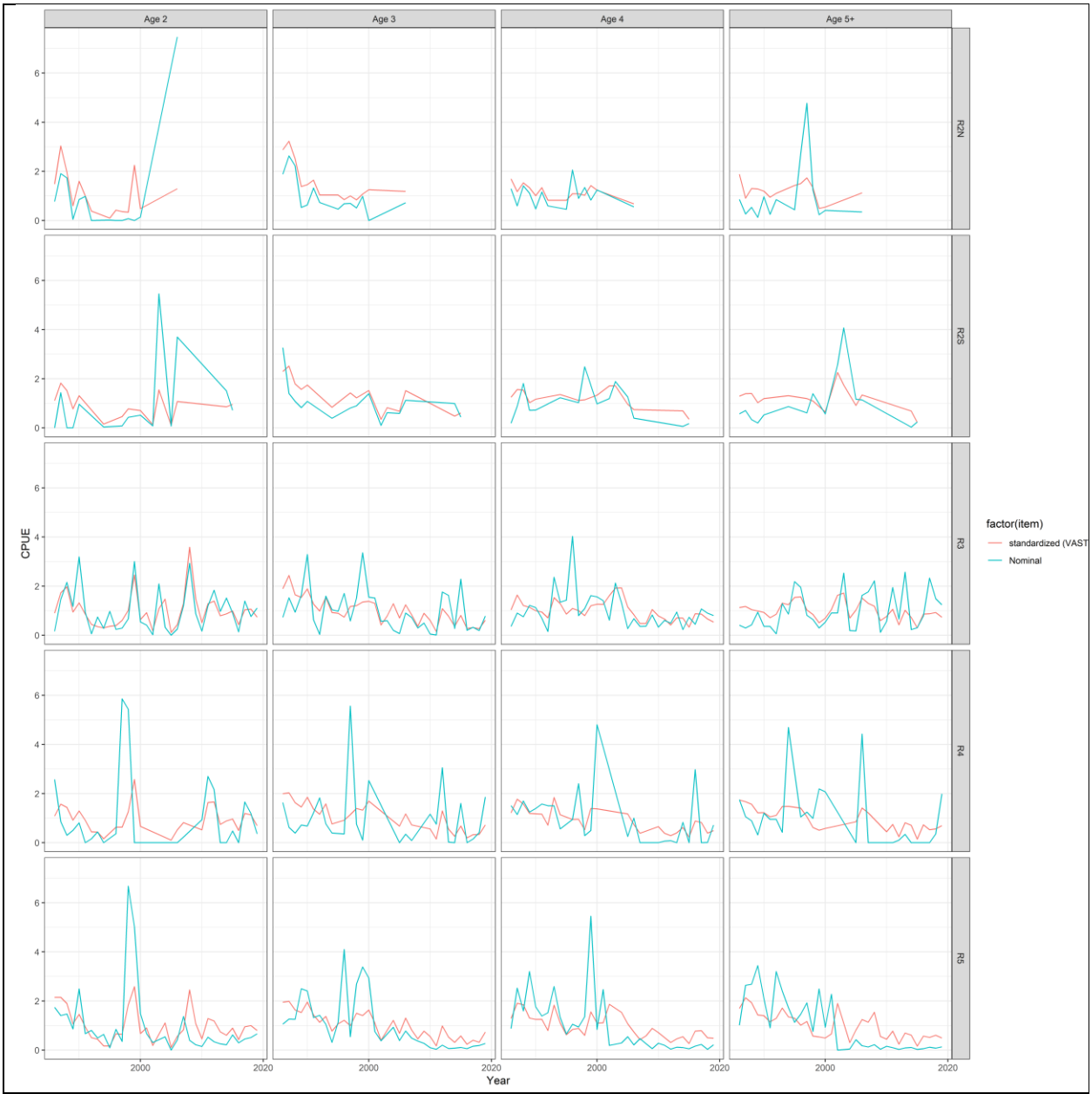

Fig. 6. Comparison of nominal (green line) and standardized (red line) year based CPUE by region (R2N, R2S, R3, R4 and R5) and by age (age 2, 3, 4 and 5+) of the age specific model (VC model) from 1986-2019.

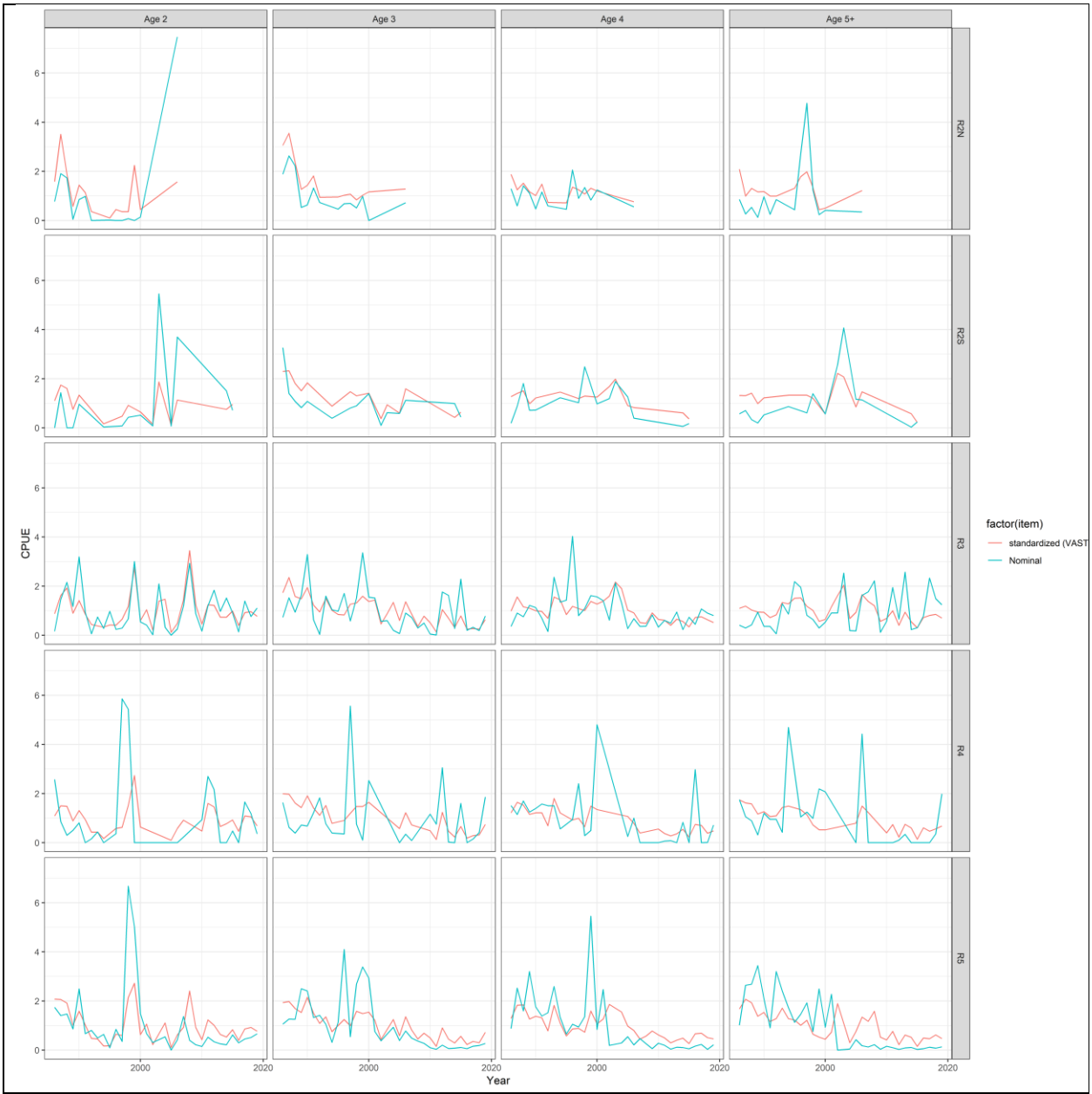

Fig. 7. Comparison of nominal (green line) and standardized (red line) year based CPUE by region (R2N, R2S, R3, R4 and R5) and by age (age 2, 3, 4 and 5+) of the age specific model (V model) from 1986-2019.

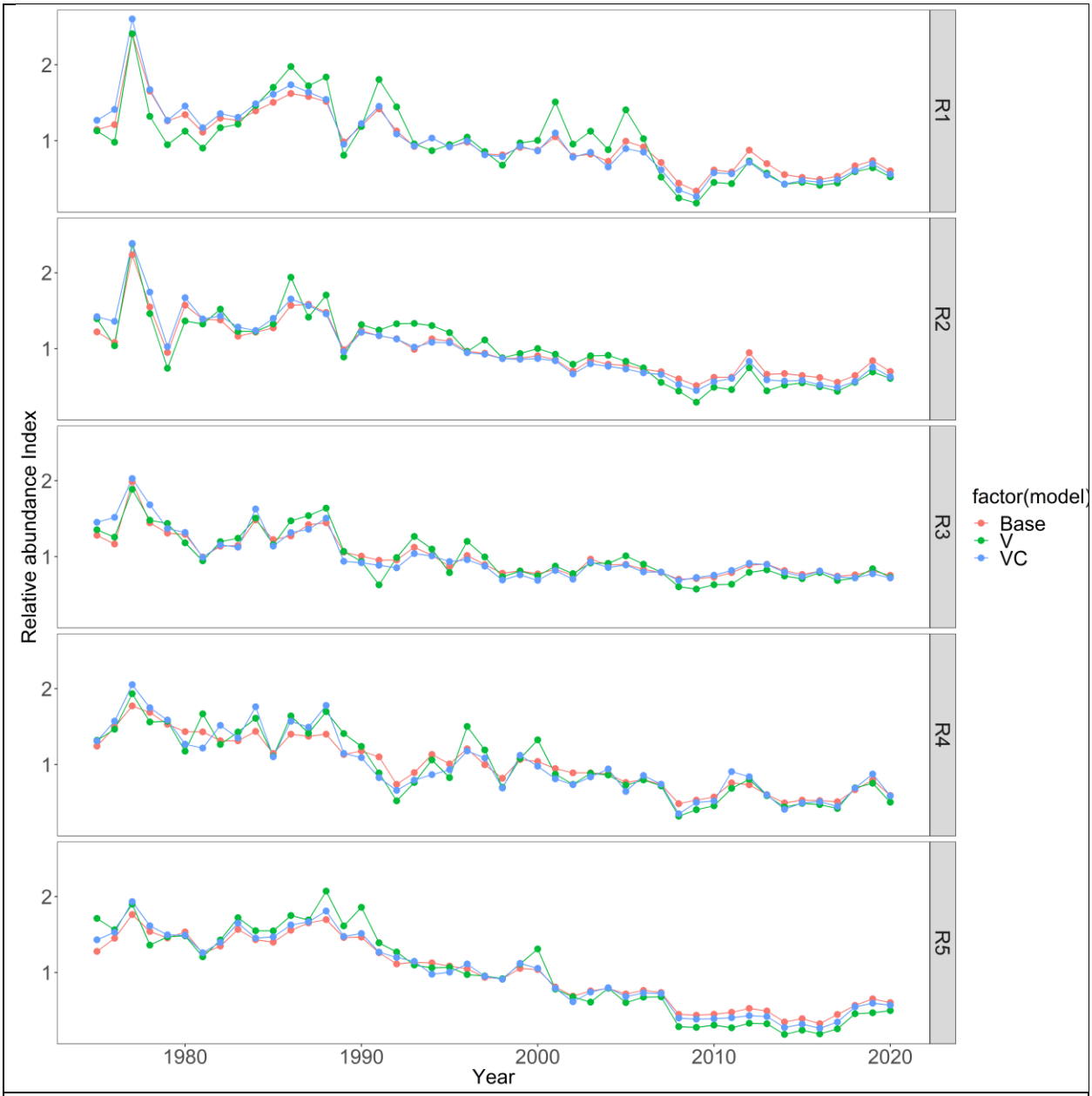

Fig. 8. Comparison of time series of abundance index by region among the age aggregated models. Base model; red, VC model; blue, V model; green

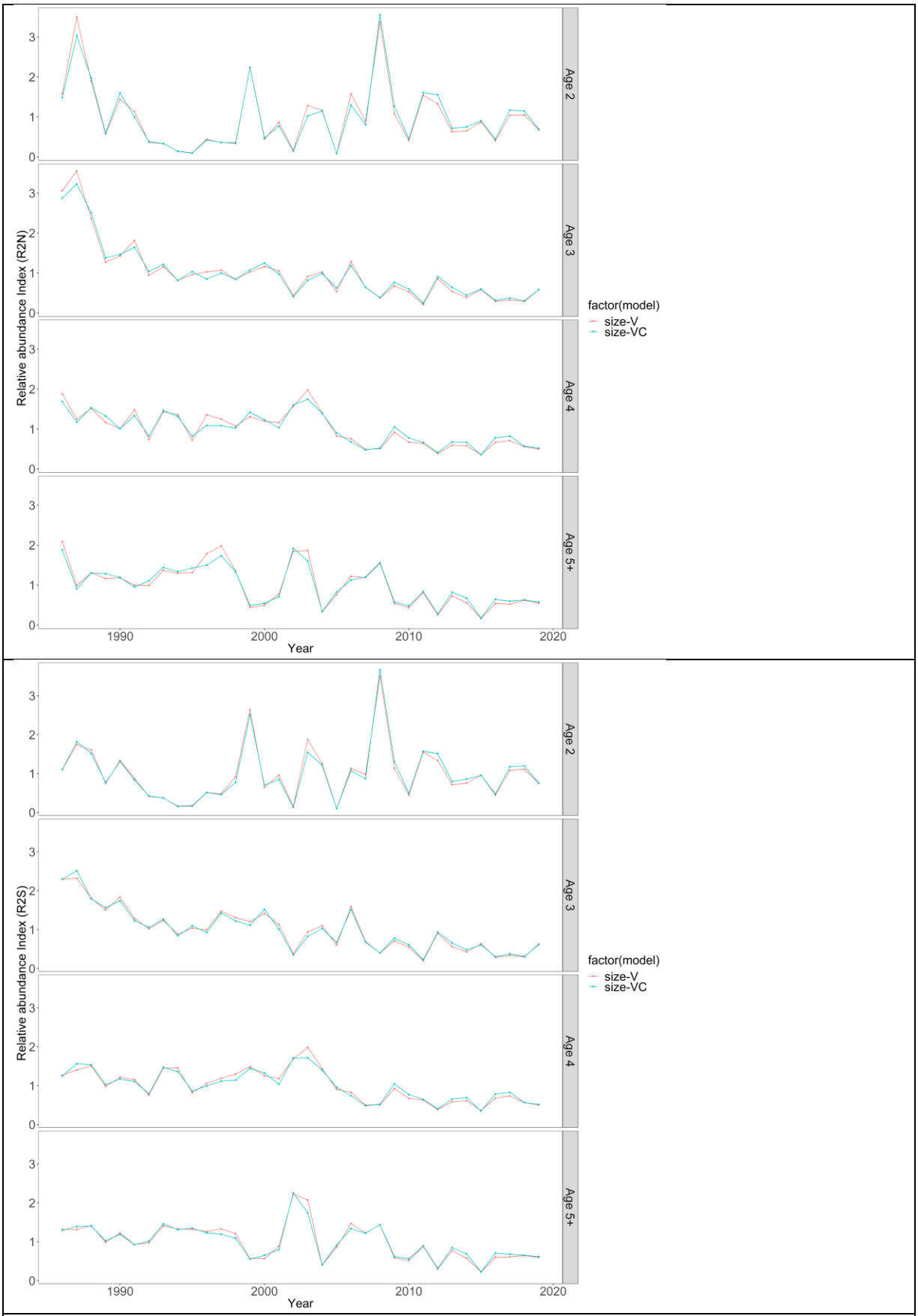

Fig. 9. Comparison time series by region and by age among the age specific models.
VC model; green, V model; red

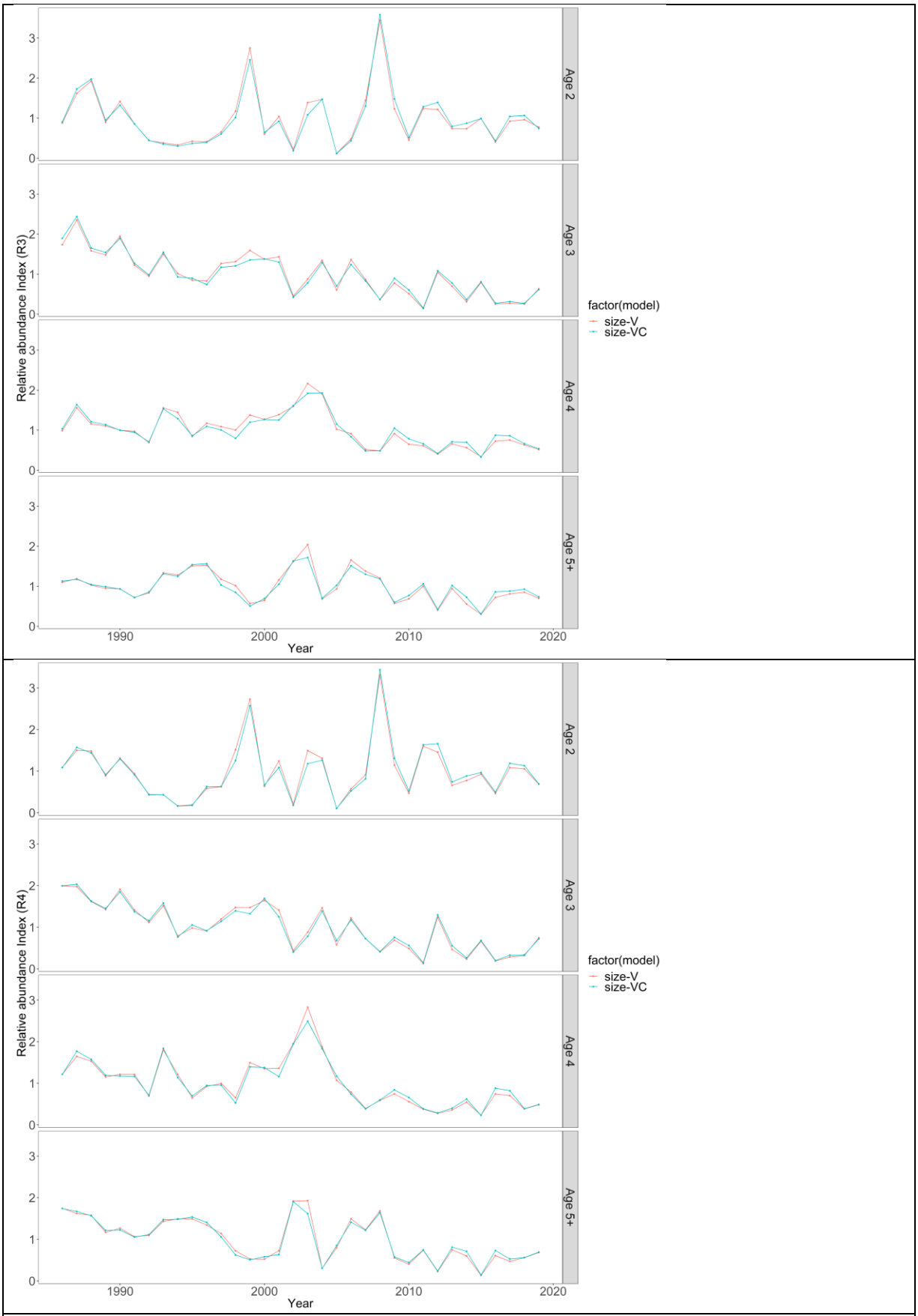

Fig. 9 (Continued). Comparison time series by region and by age among the age specific models.
VC model; green, V model; red

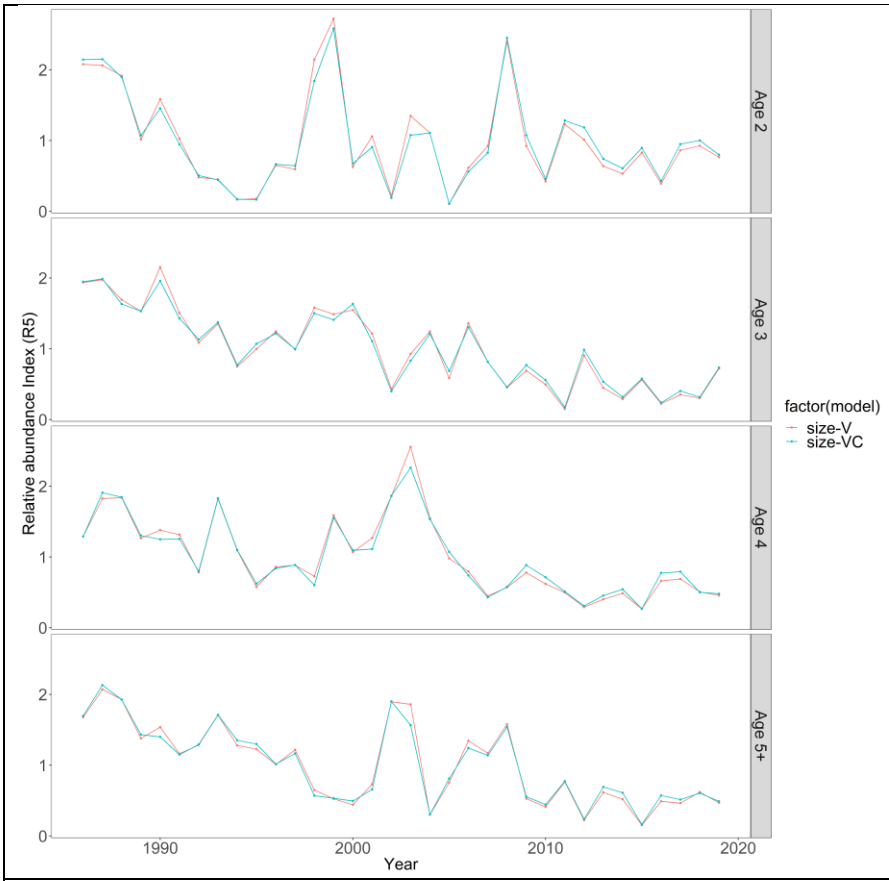

Fig. 9 (Continued). Comparison time series by region and by age among the age specific models.
VC model; green, V model; red

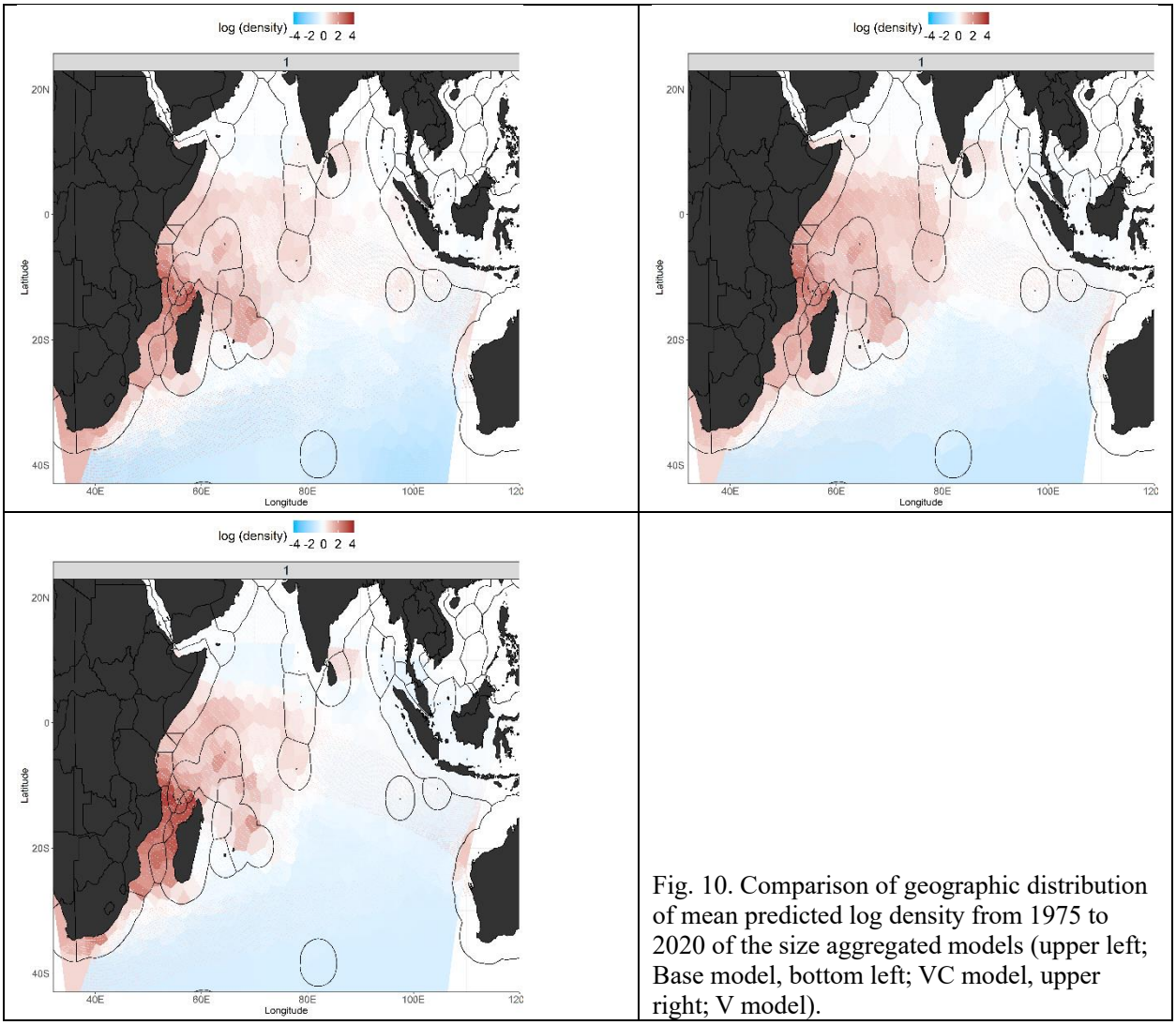

Fig. 10. Comparison of geographic distribution of mean predicted log density from 1975 to 2020 of the size aggregated models (upper left; Base model, bottom left; VC model, upper right; V model).

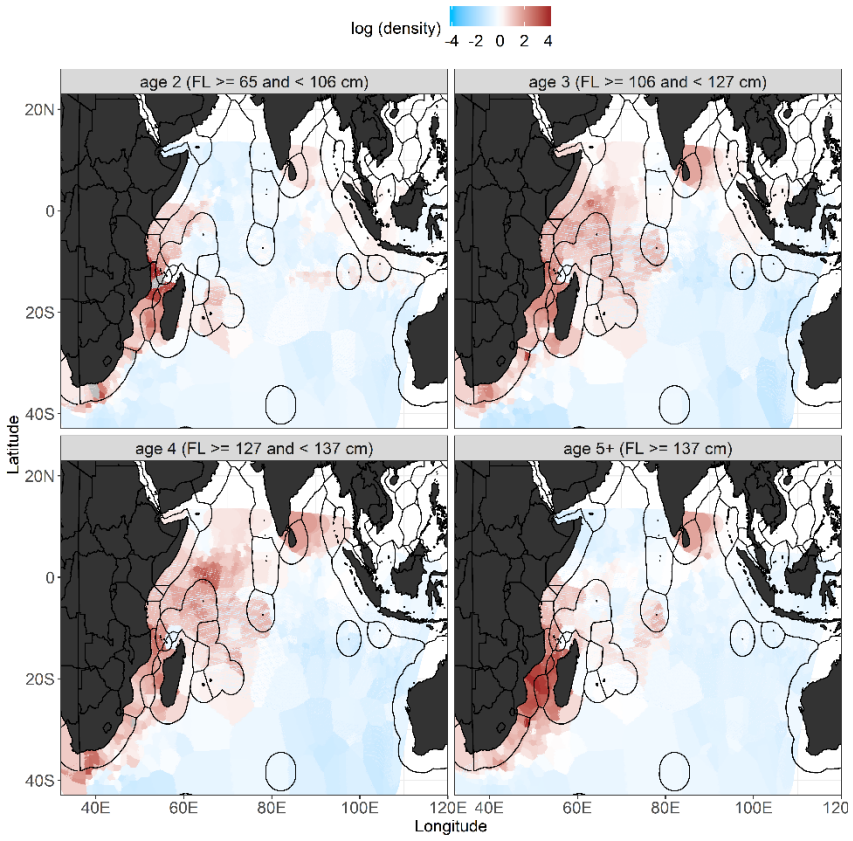

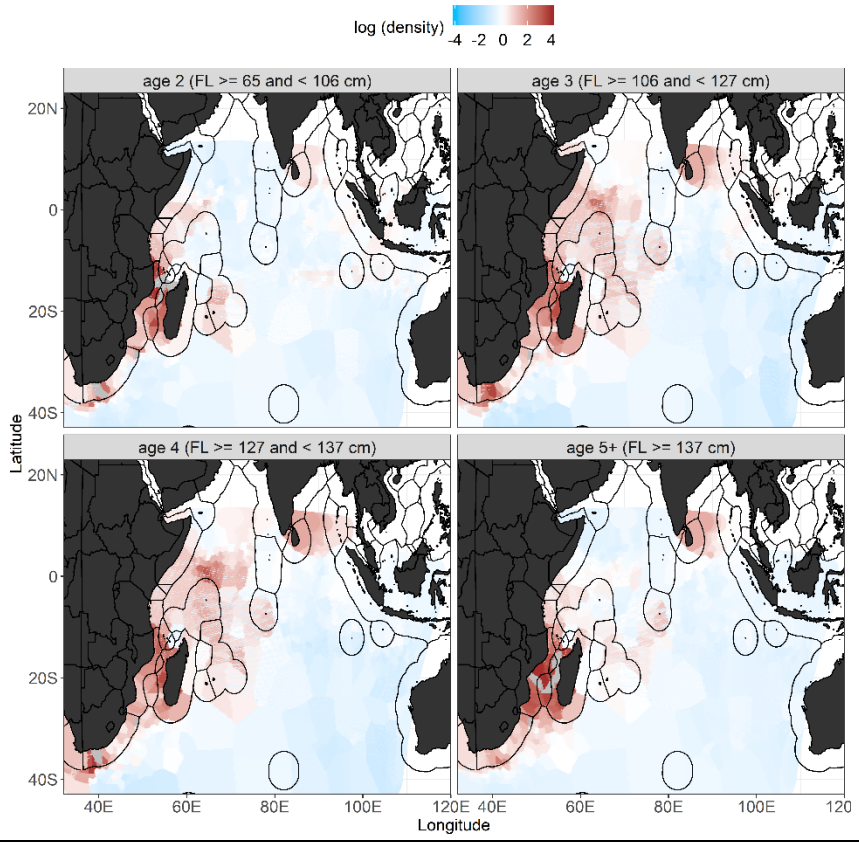

Fig. 11. Comparison of geographic distribution of mean predicted log density from 1986 to 2019 of the size specific models (upper; VC model, bottom; V model).

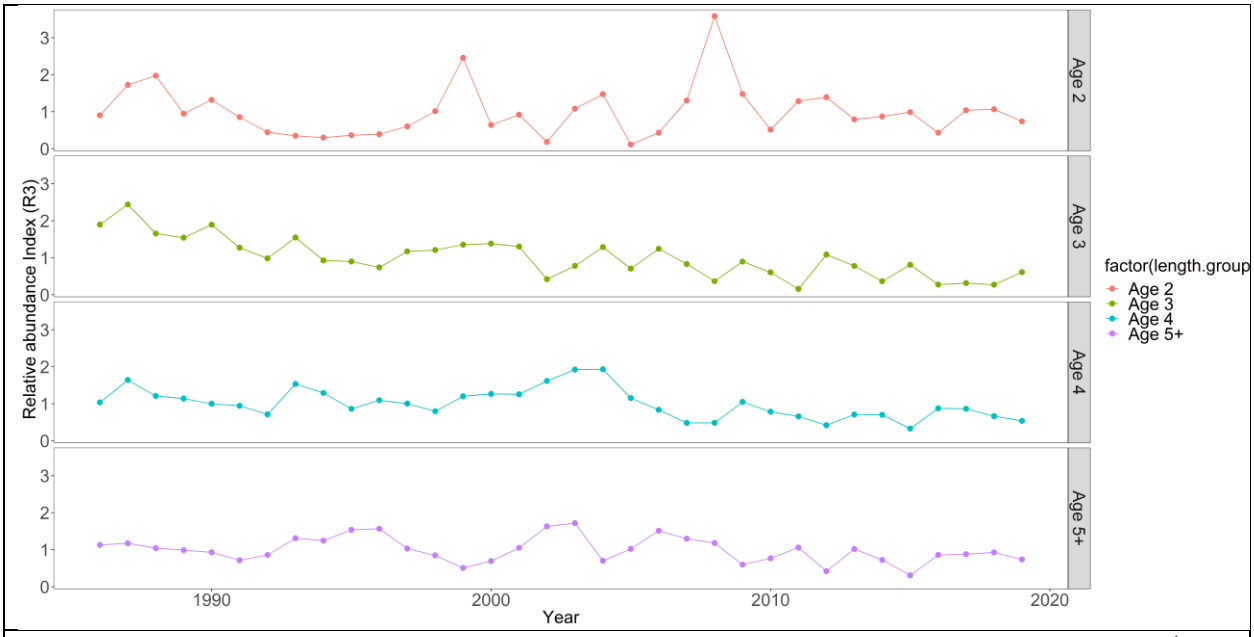

Fig. 12. Comparison of time series of standardized CPUE by age of the size specific model (size-VC model) in the region R3.